An Aqueous Reduction Method To Synthesize Spinel-$LiMn_2O_4$ Nanoparticles as a Cathode Material for Rechargeable Lithium-Ion Batteries

V. Ganesh Kumar,[†] J. S. Gnanaraj,[†] S. Ben-David,[†] David M. Pickup,[‡] Ernst R. H. van-Eck,[‡] A. Gedanken,[†] and D. Aurbach*,[†]

Department of Chemistry, Bar-Ilan University, Ramat-Gan, 52900 Israel, and Center for Materials Research, School of Physical Sciences, University of Kent, Canterbury, Kent CT2 7NR, United Kingdom

Received March 31, 2003. Revised Manuscript Received June 18, 2003

A new synthetic method has been developed and demonstrated for the utilization of commercially cheap MnO_2 for the production of nanoparticles of $LiMn_2O_4$ spinel as a cathode material for Li-ion batteries. The process involves the insertion of lithium into electrolytic manganese dioxide (EMD) in an aqueous medium with glucose as a mild reductant in open air. The material resulting from calcination is pure, spinel-structured $Li_{0.96}Mn_2O_4$ particles of sub-micrometric and nanometric size that exhibit promising electrochemical behavior in nonaqueous Li-salt solutions. Further development of this process may be interesting for the commercial production of $LiMn_2O_4$ for Li-ion batteries.

I. Introduction

Rechargeable Li-ion batteries have become a commercial reality in recent years. They are incorporated in mobile electronic equipment, such as cellular phones. The global projections for the marketing of portable electronic devices with extraordinary capabilities create a very strong driving force for R&D of light, efficient, reliable, environmentally friendly, and cheap rechargeable Li-ion batteries.[1,2]

The cathode materials for Li-ion batteries are usually oxides of transition metals due to their high electrochemical potentials during highly reversible lithium insertion/deinsertion. A huge amount of literature is available on the preparative, structural, and electrochemical studies of oxides of Co, Ni, Mn, and V with regard to lithium battery cathodes.[3] Recently, nanoparticles have been suggested as electrode materials for Li batteries.[4−6] Possible advantages of nanoparticles as active mass in electrodes for Li batteries may relate to high rate capability. Since the rate-determining step in Li insertion electrodes is supposed to be solid-state diffusion (Li ions in the bulk of the active mass), the smaller the particles, the smaller is the diffusion length, and the electrode's kinetics are expected to be faster.

The utility of MnO_2 compounds in lithium rechargeable batteries was discussed extensively in the past and has also been demonstrated in commercial rechargeable lithium batteries.[7,8] After a decade of stagnation, once again a special form of lithium manganese oxide with a nominal composition of $LiMn_2O_4$ possessing an AB_2O_4-spinel structure has emerged as a promising future candidate for cathode material in Li-ion batteries.[9−12] Reversible Li insertion around 4.1 V (vs Li/Li^+), abundance of manganese in the earth's crust, and relatively low toxicity are the advantages of the $LiMn_2O_4$ spinel as compared to lithiated cobalt and nickel oxides.

All the synthetic routes leading to the formation of spinel-$LiMn_2O_4$ published so far include a calcination step around 800 °C for many hours as a major and critical step. Almost all of them produce microparticles.[13−15] Synthesis of $LiMn_2O_4$ from MnO_2 and Li sources may also produce other Li−Mn−O compounds

* To whom correspondence should be addressed. E-mail: aurbach@mail.biu.ac.il.

† Bar-Ilan University.

‡ University of Kent.

(1) Tarascon, J. M.; Armand, M. *Nature* **2001**, *414*, 359.

(2) Tanaka, T.; Ohta, K.; Arai, N. *J. Power Sources* **2001**, *97−98*, 2. Hamlen, R.; Au, G.; Brundage, M.; Hendricks, M.; Plichta, E.; Slane, S.; Barbarello, J. *J. Power Sources* **2001**, *95−98*, 22. Marsh, R. A.; Vukson, S.; Surampudi, S.; Ratnakumar, B. V.; Smart, M. C.; Manzo, M.; Dalton, P. J. *J. Power Sources* **2001**, *97−98*, 25.

(3) Thackeray, M. M.; Ohzuku, T. *Handbook of Battery Materials*; Besenhard, J. O., Ed.; Wiley-VCH: New York, 1999; Chapter: Li-Ion Batteries.

(4) McGraw, J. M.; Perkins, J. D.; Zhang, J. G.; Liu, P.; Parilla, P. A.; Turner, J.; Schulz, D. L.; Curtis, C. J.; Ginley, D. S. *Solid State Ionics* **1998**, *115*, 407.

(5) Zhu, J. J.; Lu, Z. H.; Aruna, S. T.; Aurbach, D.; Gedanken, A. *Chem. Mater.* **2000**, *12*, 604.

(6) Sides, C. R.; Li, N. C.; Patrissi, C. J.; Scrosati, B.; Martin, C. R. *Mater. Res. Soc. Bull.* **2002**, *27*, 604.

(7) Levi, E.; Zinigrad, E.; Teller, H.; Levi, M. D.; Aurbach, D.; Mengeritsky, E.; Elster, E.; Dan, P.; Granot, E.; Yamin, H. *J. Electrochem. Soc.* **1997**, *144*, 4133.

(8) Powers, R. A. *Proc. IEEE* **1995**, *83*, 687.

(9) Product of Moli energy, Canada: http://www.molienergy.bc.ca/specs/IMR18650C.pdf.

(10) Wan, C. Y.; Nuli, Y.; Zhuang, J. H.; Jiang, Z. Y. *Mater. Lett.* **2002**, *56*, 357.

(11) Amatucci, G.; Tarascon, J. M. *J. Electrochem. Soc.* **2002**, *149*, K31.

(12) Yamane, H.; Saitoh, M.; Sano, M.; Fujita, M.; Sakata, M.; Takada, M.; Nishibori, E.; Tanaka, N. *J. Electrochem. Soc.* **2002**, *149*, A1514.

(13) Manev, V.; Banov, B.; Momchilov, A.; Nassalevska, A. *J. Power Sources* **1995**, *57*, 99.

(14) Pistoia, G.; Antonini, A.; Zane, D.; Pasquali, M. *J. Power Sources* **1995**, *56*, 37.

(15) Manev, V.; Momchilov, A.; Nassalevska, A.; Sato, A. *J. Power Sources* **1995**, *54*, 323.

10.1021/cm030104j CCC: $25.00
Published on Web 10/02/2003

as impurities.[16,17] Since the theoretical capacity of this material is not too high (practically 120−140 mA·h/g), it is extremely important to obtain by synthesis as pure an active material as possible In this paper we report on an easy, effective, and environmentally friendly method to synthesize highly pure spinel-$LiMn_2O_4$ in large amounts in a simple reaction, utilizing electrolytic manganese oxide and lithium hydroxide, which are the cheapest manganese and lithium sources, and glucose, which is a mild reductant.

II. Experimental Section

In a typical synthesis, 75.4 g of lithium hydroxide (Aldrich) was dissolved in 3 L of double-distilled water in a 10-L beaker. To this solution, 156.6 g of electrolytic manganese dioxide (EMD) was added and the resulting slurry was stirred for 1 h at 80 °C. Then 7.5 g of glucose dissolved in 500 mL of water was added while stirring was in progress, followed by the addition of 4 L of water. The stirring (reaction) was continued further for 8 h at 80 °C. At the end, the reaction slurry was 7.5 L and allowed to cool and settle for 12 h. The solid product was washed several times with pure water and then dried at 120 °C. The powder was calcined at 775 °C for 24 h in porcelain dishes.

The lithium content in the solid product was analyzed by atomic absorption (AA, Perkin-Elmer Inc.) with monochromatic radiation ($\lambda = 670$ nm). The solutions for the AA analysis were prepared by dissolving 100 mg of the powdered sample in 100 mL of 25% HCl solution and a few drops of H_2O_2, which ensured the formation of a homogeneous solution.

Differential scanning calorimetry (DSC) data were obtained using a Mettler DSC 25 (TC15 TA controller) instrument in the temperature range of 30−550 °C at a scan rate of 10 °C/min. The thermal stability of the material was analyzed using a Mettler TGA (TGA/SDTA-851E) instrument in the temperature range of 30−1030 °C at a scan rate of 10 °C/min. Powder X-ray diffraction measurements were performed on a Rigaku X-ray diffractometer (Co Kα radiation, $\lambda = 1.7920$ Å), employing well-ground samples at a scan rate of 0.5°/min to obtain precise diffraction patterns with appropriate intensities. TEM micrographs were recorded using a JEOL-JEM 100 SX electron microscope. ^{6}Li MAS NMR spectra were acquired on a Chemagnetics CMX300 Infinity spectrometer using a Chemagnetics 4-mm double-bearing probe. Data were collected at 44.2 MHz under MAS at 13 kHz with a recycle delay of 0.2 s. The delay was sufficient to prevent saturation. A rotor-synchronized 90°−τ−180° echo sequence was applied. All the spectra were referenced externally to LiOH (0 ppm). The BET-surface area measurements were carried out in a Quantachrome Instrument (Autosorb-1)−Gas Sorption System. The Li content of the samples was determined using a Perkin-Elmer atomic absorption spectrometer (AAS) with a Li lamp (Beckman) operating at $\lambda = 670$ nM. For the analysis, the particles were dissolved in an acidic solution containing HCl and H_2O_2.

Electrochemical tests, which included cyclic voltammetry and galvanostatic charge−discharge of pristine EMD, an as-synthesized Li−Mn−O phase and a calcined Li−Mn−O phase, were carried out with electrodes mounted on coin cells operating at 30 °C using Solartron and Maccor computerized electrochemical systems, respectively. Electrode mixtures were prepared by mixing 70% oxide powder, 5% carbon black, 15% graphite-KS6 (Timrex, Inc. and 10% PVDF binder (Solvey Inc.) in a 1-methylpyrrolidone solvent. A few drops of the resulting thick suspension were spread uniformly on roughened aluminum foil and dried at 120 °C for 3 h. Circular coins of 14-mm diameter were carved out of the foil, which usually possessed an effective active mass of 11 mg of spinel-$LiMn_2O_4$. Coin cells (standard 2032 type from NRC Canada) were constructed with the above cathodes in the following configuration in a glovebox maintained at a highly pure Ar atmosphere with <2 ppm of oxygen and moisture. The cell configuration was an oxide working electrode | 1 M $LiPF_6$ in an EC:DEC:DMC 2:1:2 electrolyte solution soaked in a porous polypropylene separator | Li-metal counter electrode. Electrolyte solutions based on $LiPF_6$ were obtained from Merck KGaA.

III. Results and Discussion

The stoichiometry of the solid reaction product of MnO_2, LiOH, and glucose in an aqueous medium was found to be $Li_{0.96}Mn_2O_4$ for the material washed and dried prior to calcination. The clear filtrate of the slurry obtained when 5 g of the sample was shaken with 100 mL of water showed no lithium content, thus confirming that the washing was completely effective in removing all the loosely bound surface lithium on the particles. Finally, the composition remained close to $LiMn_2O_4$ after calcination at 775 °C.

Typical DSC data of the as-prepared material displayed in Figure 1 show a broad endothermic peak around 220 °C, which corresponds to evaporation of occluded water molecules inside the pores of the Li−Mn−O material. Additionally, it indicates that the material has no amorphous fraction.[18,19]

Typical TGA data of the Li−Mn−O material produced are presented in Figure 2. They show a first weight loss of ∼4% around 220 °C, which is attributed to the evaporation of occluded water molecules followed by a second weight loss of ∼3% around 550 °C, which is due to the decomposition of organic impurities, which are probably the products of glucose oxidation that remain absorbed to the Li−Mn−O compound. The weight loss between 700 and 900 °C is a complex thermal process that includes the crucial formation step for spinel-structured $LiMn_2O_4$ between 750 and 800 °C. The synthesis temperature for the formation of pure crystallites of single-phase spinel-$LiMn_2O_4$ was optimized at 775 °C.

The powder XRD pattern of the electrolytic manganese dioxide (EMD) shown in Figure 3a correlates with the reported pattern of γ-MnO_2. The patterns reveal that the material is poorly crystalline without the proportional expected intensities arising out of the *hkl* planes. This is a usual feature of commercially available EMD materials that is widely used in primary batteries. There are several possible defects in EMD, which include the intergrowth of γ- and β-MnO_2.[20] The particles or crystallites of this EMD as shown by the TEM micrograph in Figure 4a have sizes ranging between 10 and 100 nm with a wide distribution, which results in the BET-surface area of ∼37.6 m^2/g, which may facilitate chemical Li intercalation into this material.

The powder XRD pattern of the as-synthesized Li−Mn−O phase, which possesses the composition of $Li_{0.48}MnO_2$, is shown in Figure 3b. The pattern is very similar to that of the above-discussed pristine EMD, but with some small shifts in a few peaks. This feature confirms that lithium intercalation has occurred in the

(16) Siapkas, D. I.; Mitsas, C. L.; Samaras, I.; Zorba, T. T.; Moumouzias, G.; Terzidis, D.; Hatzikraniotis, E.; Kokkou, S.; Voulgaropoulos, A.; Paraskevopoulos, K. M. *J. Power Sources* **1998**, *72*, 22.
(17) Ahn, D.; Song, M. *J. Electrochem. Soc.* **2000**, *147*, 874.
(18) Suslick, K. S.; Choe, S. B.; Cichowlas, A. A.; Grinstaff, M. W. *Nature* **1991**, *353*, 414.
(19) Koltypin, Y.; Katabi, G.; Cao, X.; Prozorov, R.; Gedanken, A. *J. Non-cryst. Solids* **1996**, *201*, 159.
(20) Schilling, O.; Dahn, J. R. *J. Appl. Cystallogr.* **1998**, *31*, 396.

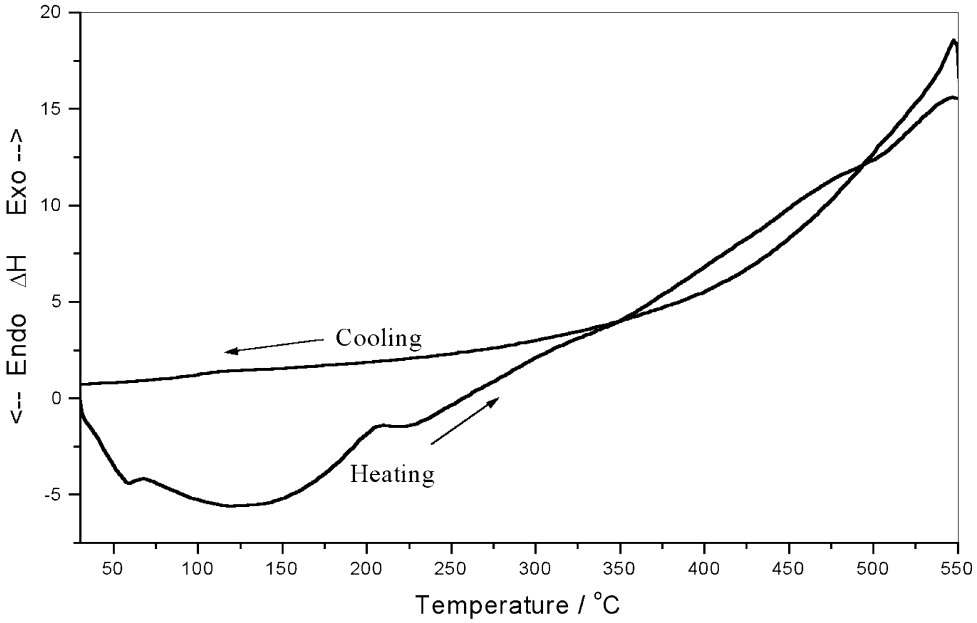

Figure 1. DSC data of the as-synthesized Li−Mn−O material.

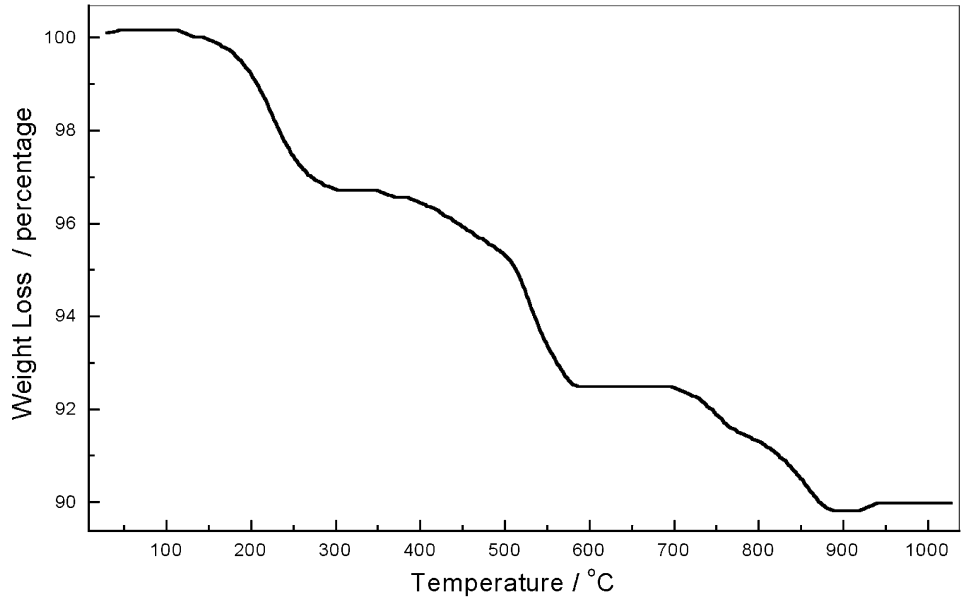

Figure 2. TGA data of the as-synthesized Li−Mn−O material.

EMD in a topotactic manner without much disturbance in its structure. The particles of this as-synthesized material, as shown in Figure 4b, are much smaller (ca. 10 nm) when compared to those of pristine EMD. This great reduction in particle size, which is further confirmed by the increase in the BET-surface area of 47.7 m^2/g, is due to the rupture and breakage of particles during the hot-turbulent intercalation reaction.

The powder XRD pattern of the calcined material, which has the composition of $Li_{0.47}MnO_2$, is shown in Figure 3c. The patterns match excellently those of the well-known spinel-$LiMn_2O_4$, with appropriate *hkl* reflections and intensities with no impurities. Hence, this calcined material should be appropriately renamed as $Li_{0.94}Mn_2O_4$. The lattice constant of this material, which is crystallized in an *Fd*3*m* space group, is calculated to be 8.23 Å. TEM micrographs of this well-crystallized spinel are shown in Figure 4c. They show the material to consist of particles in the range of 50−120 nm with some agglomeration, which causes the material to possess a small BET-surface area of 2.3 m^2/g.

The ^{6}Li MAS NMR spectrum of the calcined sample is shown in Figure 5. The three resonances are assigned according to the literature.[21,22] The main peak at about 530 ppm is assigned to lithium ions in the tetrahedral 8a site of the spinel structure; the small resonances at about 580 and 615 ppm are assigned to lithium present in the proximity of electronic defects associated with higher oxidation state manganese ions (Mn^{4+}). The origin of these electronic defects is thought to be the trapping of Mn^{4+} charges around lattice defects (i.e., Mn 16d vacancy or Li-for-Mn substitutions). The important feature of this spectrum is that the intensity arising from defects is very low compared to that of usual

(21) Lee, Y. J.; Wang, F.; Grey, C. P. *J. Am. Chem. Soc.* **1998**, *120*, 12601.
(22) Tucker, M. C.; Reimer, J. A.; Cairns, E. J. *Electrochem. Solid State Lett.* **2000**, *3*, 463

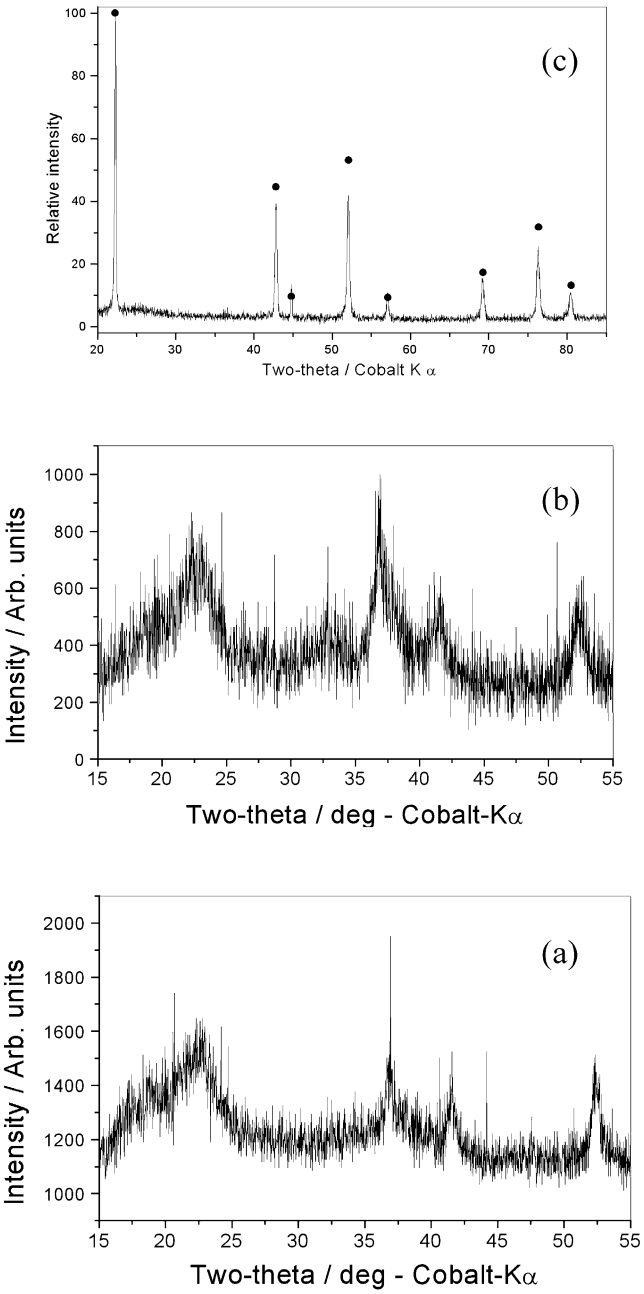

Figure 3. (a) Powder XRD patterns of the pristine EMD. (b) Powder XRD patterns of the as-synthesized Li−Mn−O material. (c) Powder XRD patterns of the calcined material ($LiMn_2O_4$ spinel).

$LiMn_2O_4$ materials[21] and the "main" spinel peak (530 ppm) is very narrow. Hence, we can conclude that the material synthesized herein is very pure and uniform.

A cyclic voltammogram in the potential range 2.5−4.3 V vs Li/Li^+ of the as-synthesized Li−Mn−O material in a $LiPF_6$ solution is shown in Figure 6. The voltammogram shows a reversible activity centered around 3 V, which is due to lithium deinsertion and insertion. This is anticipated for poorly ordered Li−Mn−O phases.[23] This phase also shows some activity in the higher voltage regime around the 4-V range, much different from that expected for the spinel $LiMn_2O_4$.[24] In addition

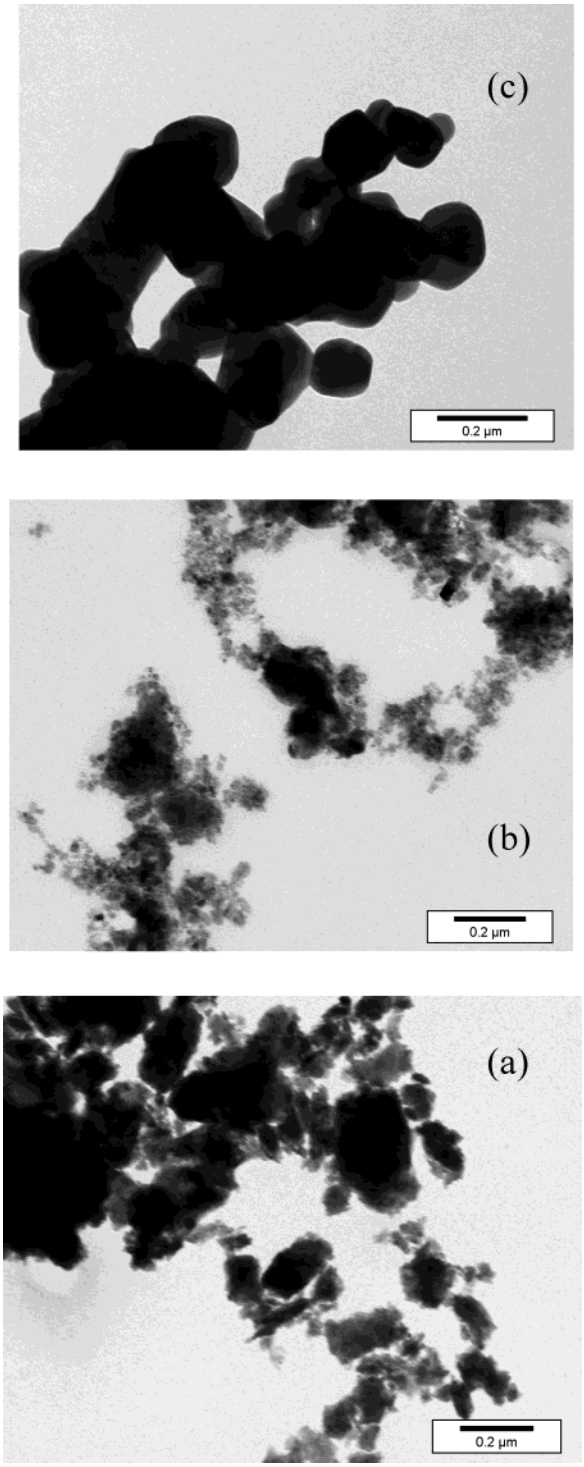

Figure 4. (a) A TEM micrograph of pristine EMD. A scale appears in the picture. (b) A TEM micrograph of as-synthesized Li−Mn−O material. A scale appears in the picture. (c) A TEM micrograph of calcined material. A scale appears in the picture.

to the XRD characterization (Figure 5b), the electrochemical measurements confirm the absence of any spinel phase in the as-synthesized material.

Fresh electrodes of as-synthesized Li−Mn−O and pristine EMD possessing a similar amount of active masses were fabricated and tested for their reversible lithium insertion−deinsertion properties restricted to 2.5−3.5 V vs Li/Li^+, to evaluate the relative performance of the reaction product over the pristine MnO_2 material.

(23) Myung, S. T.; Komaba, S.; Kumagai, N. *Electrochem. Acta* **2002**, *47*, 3287.
(24) Choi, S.; Manthiram, A. *J. Electrochem. Soc.* **2002**, *149*, A1157.

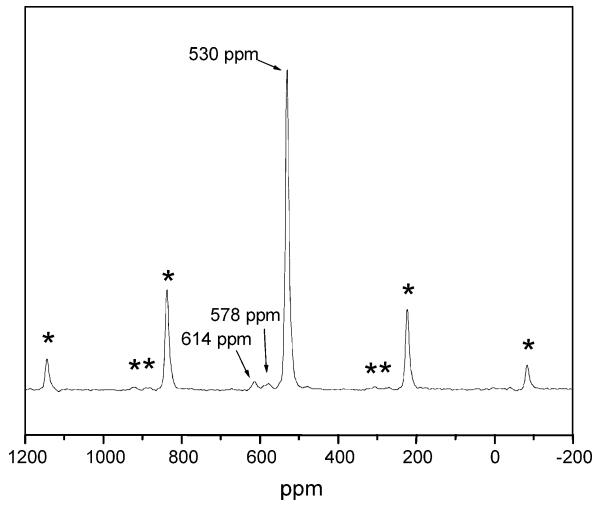

Figure 5. ^{6}Li NMR spectrum of the calcined material (∗ refers to the spinning sidebands).

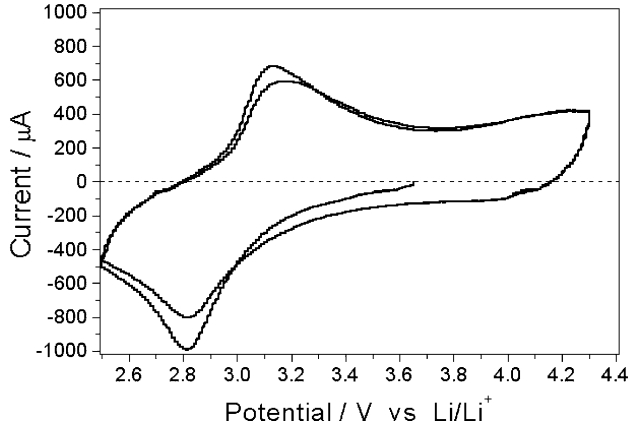

Figure 6. Cyclic voltammograms of as-synthesized Li−Mn−O material in the potential range 2.5−4.3 V vs Li/Li^+ (two cycles). EC-DEC-DMC 2:1:2/1 M $LiPF_6$, 1 mV/s.

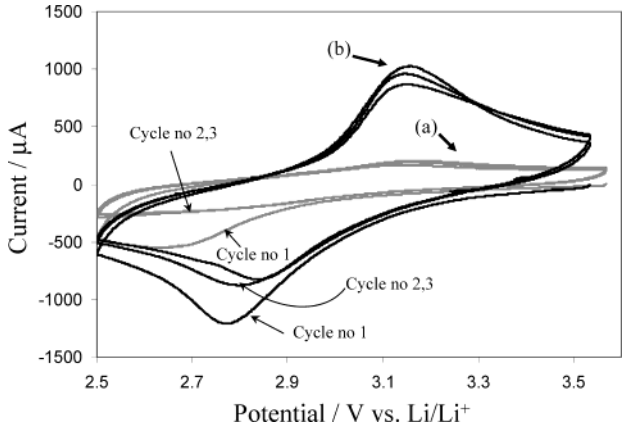

Figure 7. Cyclic voltammograms of (a) pristine EMD and (b) as-synthesized Li−Mn−O 2.5−3.5 V (first three cycles). EC-DEC-DMC 2:1:2/1 M $LiPF_6$, 1 mV/s.

The cyclic voltammograms of the two materials for the first three cycles are shown in Figure 7a,b, as indicated. The CV of as-synthesized Li−Mn−O shows expected reversible electrochemical activity with a gradual decrease in the peak currents during cycling. The CV of pristine EMD electrodes show very low peak currents, reflecting its lower initial activity in comparison with that of the Li−Mn−O phase. This diagnostic feature shows that the EMD is converted to a more useful form

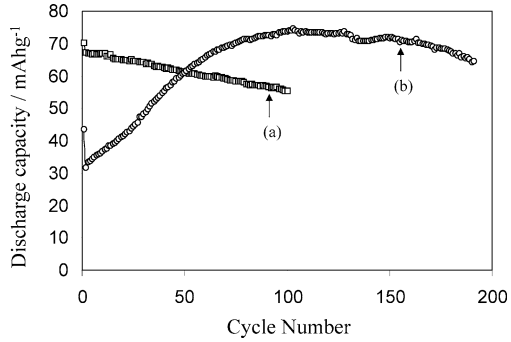

Figure 8. Cycle life data of (a) as-synthesized Li−Mn−O and (b) pristine EMD material during galvanostatic cycling in the 3-V region, at a C/10 rate. EC-DEC-DMC 2:1:2/1 M $LiPF_6$.

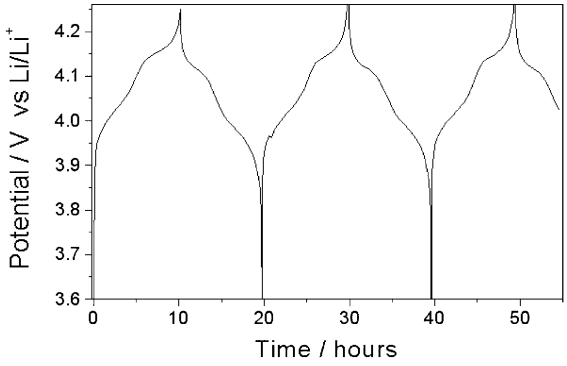

Figure 9. Typical galvanostatic profile (E vs time) of the calcined material electrode at 30 °C at a C/10 rate. EC-DEC-DMC 2:1:2/1 M $LiPF_6$,

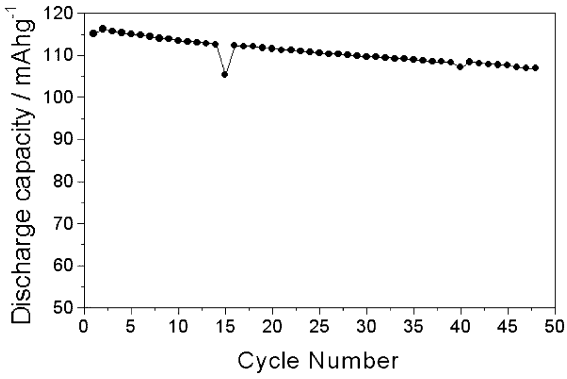

Figure 10. Cycle life data of calcined material electrode at 30 °C at a C/10 rate. EC-DEC-DMC 2:1:2/1 M $LiPF_6$,

upon the soft chemical lithium intercalation reaction described herein. The better performance of the as-synthesized material over its pristine counterpart could not be due to a bulk structural effect, as the powder XRD patterns are more or less similar. Rather, the better effect could be due to the morphological effect, as demonstrated by the TEM micrographs. The particles are greatly reduced in size during the synthesis, as compared to pristine EMD, which results in a greater mass diffusion, and hence, better activity. Another interesting feature of the pristine EMD is its large loss in capacity when going from the first to the second discharge cycle. The loss in the capacity upon the first cycle could be due to some surface modification of the EMD upon a first electrochemical lithium insertion (which occurs initially to a very low extent).

The cycle life data in the 3-V region for the as-synthesized Li−Mn−O phase along with pristine EMD

are shown in (a) and (b), respectively, of Figure 8. The as-synthesized Li−Mn−O shows a higher initial capacity of ~70 mA·h/g, which by itself is not a very attractive value in comparison with the literature results for Li_xMnO_2.[25] The comparison of the cycling behavior (Li insertion−deinsertion) between the synthesized $Li_{0.48}MnO_2$ and the pristine EMD (MnO_2) presented in Figure 8 is very interesting. Initially, the capacity of the pristine MnO_2 for Li insertion is very low, but it increases upon cycling. Within 50 repeated cycles, the capacity of electrodes comprising pristine EMD reaches a higher capacity than that of the synthesized $Li_{0.48}MnO_2$, around 70 mA·h/g. Hence, the repeated electrochemical process with EMD, which includes cathodic polarization to 2.5 V, facilitates its lithiation by reduction, due to some structural changes that we could not trace by XRD. (Note that the XRD patterns of the pristine EMD and the synthesized $Li_{0.48}MnO_2$ are similar, as seen in Figure 3.) Thus, the reduction process of MnO_2 by glucose in the presence of a Li source (aqueous LiOH) that was developed therein can be considered as an efficient lithiation process for MnO_2, which forms a host material that can serve as a very good precursor for the production of highly pure $LiMn_2O_4$ spinel.

A typical galvanostatic charged−discharge cycling process of the calcined material at a C/10 rate is shown in Figure 9, which correlates with the expected 4-V double-plateau behavior of spinel electrodes.[26−28] The cycle life data of this material are shown in Figure 10, which shows the material to possess a discharge capacity >115 mA·h/g, which slightly fades during prolonged cycling, as is usual for this material in $LiPF_6$ solutions.[11]

Conclusions

This paper describes an elegant way of producing highly pure $LiMn_2O_4$ spinel material. It was discovered that reduction of MnO_2 in the presence of a Li source (LiOH) in aqueous media using a very mild reductant, that is, glucose, produces lithiated MnO_2, which can be delithiated and lithiated electrochemically and reversibly in nonaqueous Li-salt solutions. Calcination of the $Li_{0.48}MnO_2$ thus formed, at temperatures between 750 and 800 °C, forms highly pure $LiMn_2O_4$ spinel. The latter product is formed in agglomerates of sub-micrometric cubic crystals, part of which are of nanometer size. It should be noted that commercial $LiMn_2O_4$ powers, produced by solid-state, high-temperature reactions, do not have the nearly completed cubic morphology of the $LiMn_2O_4$ synthesized in this work. Preliminary testing of this material as the active mass in composite cathodes for Li and Li-ion batteries showed that a reasonable capacity (115 mA·h/g) and stability upon cycling could be obtained. We believe that we outline herein a simple and cheap synthesis of $LiMn_2O_4$ spinel material. In addition, the morphology of the material thus obtained (sub-micrometric and nanometric crystals) looks promising for high-rate behavior. However, further optimization of the composite electrodes and further testing at elevated temperatures are needed to confirm that the $LiMn_2O_4$ material synthesized herein may be commercially important.

Acknowledgment. The authors would like to express their gratitude to the European Comission for their financial support (EC-project NNE5-1999-00395 ENK6-CT99-00006).

CM030104J

(25) Armstrong, A. R.; Bruce, P. G. *Nature* **1996**, *381*, 6582.
(26) Levi, E.; Levi, M. D.: Salitra, G.; Aurbach, D.; Oesten, R.; Heider, U. *Solid State Ionics* **1999**, *126*, 109.
(27) Xia, Y. Y.; Yoshio, M. *J. Electrochem. Soc.* **1996**, *143*, 825.
(28) Mukerjee, S.; Thurston, T. R.; Jisrawi, N. M.; Yang, X. Q.; McBreen, J.; Daroux, M. L.; Xing, X. K. *J. Electrochem. Soc.* **1998**, *145*, 466.